

Quantum-Chemical Simulation of New Hybrid Nanostructures: Small Fullerenes C_{20} and C_{28} in Single-Walled Boron–Nitrogen Nanotubes

V. V. Ivanovskaya, A. N. Enyashin, A. A. Sofronov,
Yu. N. Makurin, and A. L. Ivanovskii

Institute of Solid State Chemistry, Ural Branch, Russian Academy of Sciences, Ekaterinburg, Russia

Received April 12, 2002

Abstract—A quantum-chemical simulation of new hybrid nanostructures consisting of regular chains of the small fullerenes C_{20} and C_{28} encapsulated into the bulk of achiral zigzag single-walled boron–nitrogen nanotubes $[(C_{20}, C_{28})@BN-NT]$. The electronic properties and the nature of interatomic bonds in these nanostructures are analyzed as a function of the fullerene and the distances between fullerenes in the chain and between fullerenes and tube walls. The electronic characteristics of hybrid nanostructures are compared with those of “isolated” fullerenes and nanotubes, and $(C_{20}, C_{28}) + BN-NT$ structures simulating fullerene adsorption on tube surface as the initial stage of $(C_{20}, C_{28})@BN-NT$ formation.

Further prospects of application of nanotubes (NT) are closely related to the development of approaches to targeted modification of their properties. In this connection hybrid nanotubular structures formed by a combination of two (or several) nanometer-sized objects hold great promise [1, 2].

The first representatives of such structures are the so-called peapods consisting of fullerenes C_{60} intercalated into the bulk of single- and double-walled [3–12] carbon nanotubes ($C_{60}@C-NT$). These objects are unique nanocomposites combining two allotropic forms of carbon of different size (1D + 0D): quasi-one-dimensional (1D; nanotubes) and zero-dimensional (0D; fullerenes). It was found that carbon peapods can contain fullerenes of different size, from C_{36} to C_{120} . However, until now most emphasis has been paid to synthesis and properties of peapods containing the “classical” fullerenes C_{60} (for review, see [1]).

Experiments performed by high-resolution transmission electron microscopy [13] and first quantum-chemical calculations of $C_{60}@(n,n)C-NT$ ($n = 8–10$) systems [14, 15] gave evidence to show that introduction of fullerenes into the internal cavity of nanotubes markedly affects the electronic structure of the peapod “shell.” The resulting nanostructures acquire much different, compared with “pure” nanotubes, energetic, cohesion, conducting, and other physicochemical characteristics.

This class of unusual nanostructures with diverse

functional properties can be extended both by forming peapods on the basis of noncarbon nanotubes [2] and by using as intercalants various fullerene cage-like molecules.

Thus, more complex peapods containing endofullerenes encapsulated in carbon nanotubes were recently synthesized: $Gd@C_{80}@NT$ [12], $Dy@C_{82}@NT$ [16], and $La_2@C_{80}@NT$ [17]. Stefan *et al.* [18] reported the preparation of boron–nitrogen nanotubes (BN-NT) including four-shell (like known carbon onion structures) octahedral boron–nitrogen cage-like nanoclusters $B_{12}N_{12}@B_{76}N_{76}@B_{208}N_{208}@B_{412}N_{412}$.

In [19, 20] we proposed that the same approach is feasible for preparing new nanotubular materials involving Group III–V *d*-metals which possess a high carbide-forming capacity [21] and cannot as such be encapsulated in nanotubes. Hypothetical hybrid nanosystems comprising regular chains of stable metal–carbon nanoclusters, metal carbohedra M_8C_{12} (see the review [22]), inside nanotubes were proposed and first quantum-chemical calculations of such structures on the basis of carbon and boron–nitrogen nanotubes were performed ($M_8C_{12}@(12,0)C, BN-NT$, $M = Sc, Ti, V$) [2, 19, 20].

Experimentally [3–12], empirical correlations between the diameter of carbon nanotubes and that of intercalating fullerenes were found to reveal an optimal diameter of carbon nanotubes for forming the above hybride nanostructures (>1.3–1.4 nm).

Table 1. Parameters of unit cells simulating hybrid nanostructures $(C_{20}, C_{28})@(n,0)BN-NT$

Parameter	$C_{20}@(9,0)NT$	$C_{20}@(13,0)NT$	$C_{28}@(10,0)NT$
Number of atoms in the cell	92	124	108
Cell composition	$C_{20}B_{36}N_{36}$	$C_{20}B_{52}N_{52}$	$C_{28}B_{40}N_{40}$
Nanotube diameter, nm	0.709	0.102	0.787
Fullerene–nanotube wall distance, nm	0.155	0.311	0.155
Fullerene–fullerene distance, nm	0.454	0.454	0.206

We suggest that the small fullerenes C_{20} [23–25] and C_{28} [26–29] as potential intercalates for smaller size nanotubes. Therewith, the electronic features of the outer shells of these molecules, specifically the presence of unsaturated “outer” bonds [23–29], may cause spontaneous one-dimensional polymerization to form inside the tube (as a kind of reactor) a variety of new nanoforms of the basis of C_{20} and C_{28} dimers and trimers, oblong “nanocapsules,” etc. Certain unusual nanoforms formed by polymerization of C_{60} were observed [8–12] in $C_{60}@C-NT$ peapods where the process was induced by exposure to light, heating, or high-energy electron bombardment.

In the present work we performed quantum-chemical calculations of the electronic structure and chemical bonding in hypothetical hybride nanosystems comprising the small fullerenes C_{20} and C_{28} encapsulated into single-walled achiral zigzag $(n,0)$ boron–nitrogen nanotubes. The choice of BN-NT was defined by the fact that their electronic properties (in particular, the magnitude of the dielectric gap ΔE_g) are quite stable with respect to structural parameters of tubes (diameter and chirality [2, 30]), making BN-NT candidates for nanoelectronic.

For simulating $(C_{20}, C_{28})@(n,0)BN-NT$ ($n = 9, 10, 13$) we used unit cells whose sizes and geometric parameters are listed in Table 1. The choice of the unit cells was defined by the following reasons. In the majority of synthesized carbon peapods [3–12], the distance from C_{60} to nanotube walls are close to the so-called van der Waals gap (interplanar spacing in graphite or hexagonal BN), as well as to the distance between fullerenes in molecular crystals (fullerites) or between neighboring coaxial cylinders in multiple-walled nanotubes (~ 0.30 nm). Therefore, the first series of objects, $C_{20}@(13,0)BN-NT$, was simulated by 124-atomic cells with fullerene–nanotube distances close to the mentioned value (Table 1).

Other characteristic distances are covalent C–C (B–N) bond lengths in layers of graphite-like phases, or between neighboring atoms in fullerenes or in

nanotube walls (~ 0.142 nm). The $C_{20}@(9,0)BN-NT$ and $C_{28}@(10,0)BN-NT$ peapods with the corresponding fullerene–nanotube distances were described by 92- and 108-atomic cells.

Figure 1 exemplify a cell that simulates the $C_{20}@(9,0)BN-NT$ peapod, as well as its possible configurations I–IV with varied mutual fullerene–nanotube arrangements.

The electronic structure and chemical bonding parameters in peapods were correlated with respective values for “isolated” fullerenes, their one-dimensional chains, and tubes. Furthermore, $[C_{20}, C_{28}]_\infty + (n,0)BN-NT$ systems were considered, that comprise regular chains of fullerenes located on the outer side of nanotubes at distances corresponding to the fullerene–tube distances in $(C_{20}, C_{28})@(n,0)BN-NT$ (Table 1). These systems simulate a fullerene chain adsorbed on nanotube surface (hereinafter, ad-systems). As noted in [6–8, 11, 12], peapods are likely to be formed by a two-stage mechanism. First fullerenes are adsorbed on nanotube surface and then penetrate into the intratubular region (through open ends of the tube or through defects in its walls).

In the calculations, the structures of fullerenes and tubes were set invariant at values corresponding to those reported in [25, 29, 30]. The calculations were performed by the tight binding band structure method with EHT parametrization [19, 20].

Let us consider the formation of the electronic structure and interparticle bonds in the $C_{20}@(9,0)BN-NT$ hybride nanosystem by its sequential assembling from the starting nanostructures in the series $[C_{20}]_\infty$ chain, $(9,0)BN$ nanotube, $[C_{20}]_\infty + (9,0)BN-NT$ ad-system, and $C_{20}@(9,0)BN-NT$ hybride system (Fig. 2 presents the model densities of states of these systems).

Since the linear chain $[C_{20}]_\infty$ consists of molecules spaced at 0.454 nm which much exceeds characteristic covalent and van der Waals distances, C_{20} – C_{20} interactions are lacking, and the spectrum of the system consists of a set of discrete states corresponding to

the energy diagram of a single neutral molecule C_{20} [23–25].

The electronic structure of (9,0)BN-NT contains two bands of occupied states, $N2s$ (band *A*) and hybridized $N2p$ – $B2s,2p$ states (band *B*), separated by a wide dielectric gap ($\Delta E_g \sim 5.23$ eV) from the conductivity band (*C*). This result is nicely consistent with the estimates for ΔE_g obtained by other band structure calculations (~ 5.5 eV [30]).

The spectrum of the model ad-system $[C_{20}]_\infty + (9,0)BN-NT$ [C_{20} –(9,0)BN-NT distance 0.155 nm] differs sharply from the superposition of the model density of states for $[C_{20}]_\infty$ and (9,0)BNNT and exhibits certain features derived from interactions of outer states of fullerenes on adsorption of the latter on tube surface. This is clearly seen from the splitting of the $C2s$ -like peak (*A'*), changes in the shape of the density of states the lower and upper boundaries (*B'*, *B''*) of the hybrid $N2p$ – $B2s,2p$ band (*B*), as well as appearance of a set of new states near the dielectric gap of the tube (between bands *B* and *C*, Fig. 2).

The effects of tube–fullerene interactions still more enhance in the $C_{20}@ (9,0)BN-NT$ peapod whose model density of electronic states is presented in Fig. 2 (for cell configuration III which corresponds, according to estimates for the total one-electron energy, to the most stable state of the peapod, Table 2). In the spectrum of $C_{20}@ (9,0)BN-NT$, the fullerene states between bands *A* and *B* are additionally split; new states are formed near the upper boundary of band *B* and Fermi level (E_F). It will be emphasized that the most active in combining $[C_{20}]_\infty$ and BN-NT into quasi-one-dimensional hybrid structures are outer (partly occupied [23–25]) fullerene orbitals that form near-Fermi states of the $[C_{20}]_\infty + (9,0)BN-NT$ and $C_{20}@ (9,0)BN-NT$ systems and the chain–nanotube bond. The type of their distribution depends strongly on cell configuration (Fig. 1, Table 1).

The mentioned $[C_{20}]_\infty$ and BN-NT rearrangement effects are almost lacking in the formation of the ad-system and peapod with characteristic van der Waals bond distances: The electronic structures of $[C_{20}]_\infty + (13,0)BN-NT$ and $C_{20}@ (13,0)BN-NT$ are a superposition of the spectra of $[C_{20}]_\infty$ and BN-NT (Fig. 3). As seen, the upper, partly occupied band of the $[C_{20}]_\infty$ chain is localized near the dielectric gap of NT. Since the nanotube and C_{20} states scarcely interact, then the density of electron carriers is localized inside the BN-cylinder, whereas the nanotube as such preserves semiconducting properties.

The calculated crystal overlap orbital populations (Table 2) show that the overlap populations of B–N

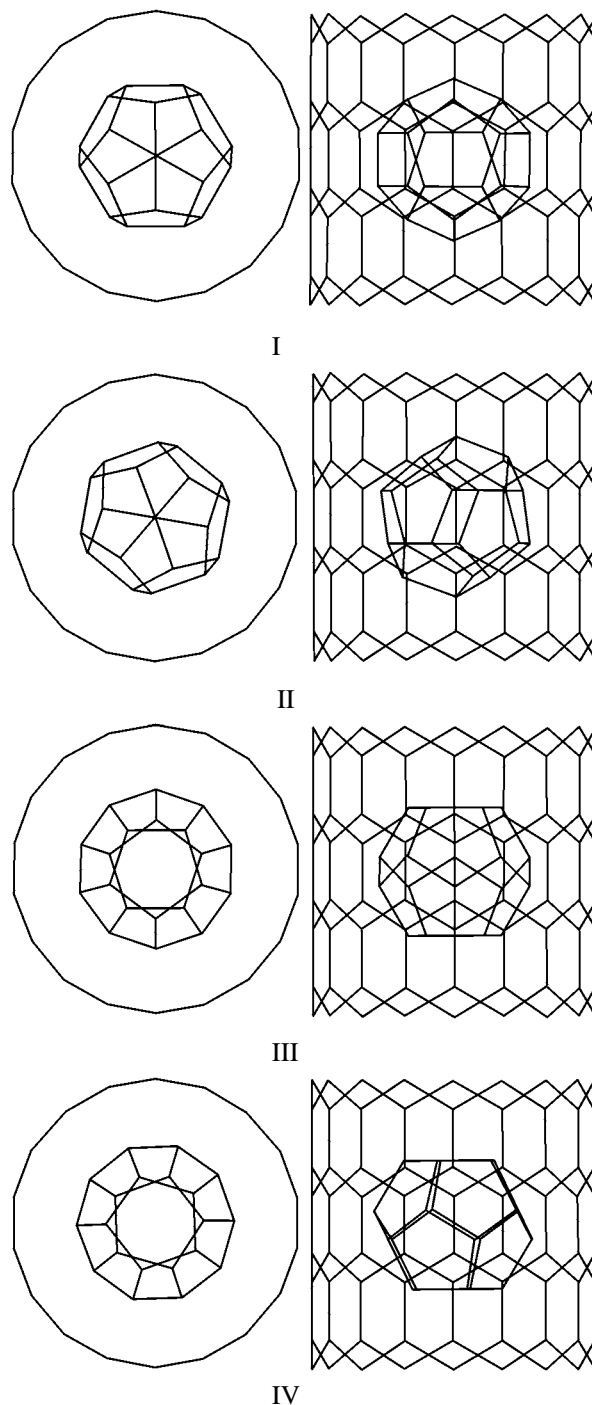


Fig. 1. Cell used in the band calculations of the electronic structure of the $C_{20}@ (9,0)BN-NT$ peapods and its possible configurations I–IV.

crystal orbitals decrease (relative to an isolated nanotube) in the series (9,0)BN-NT, $[C_{20}]_\infty + (9,0)BN-NT$, and $C_{20}@ (9,0)BN-NT$ and get different in different nanotube sections. It is seen that the C_{20} –

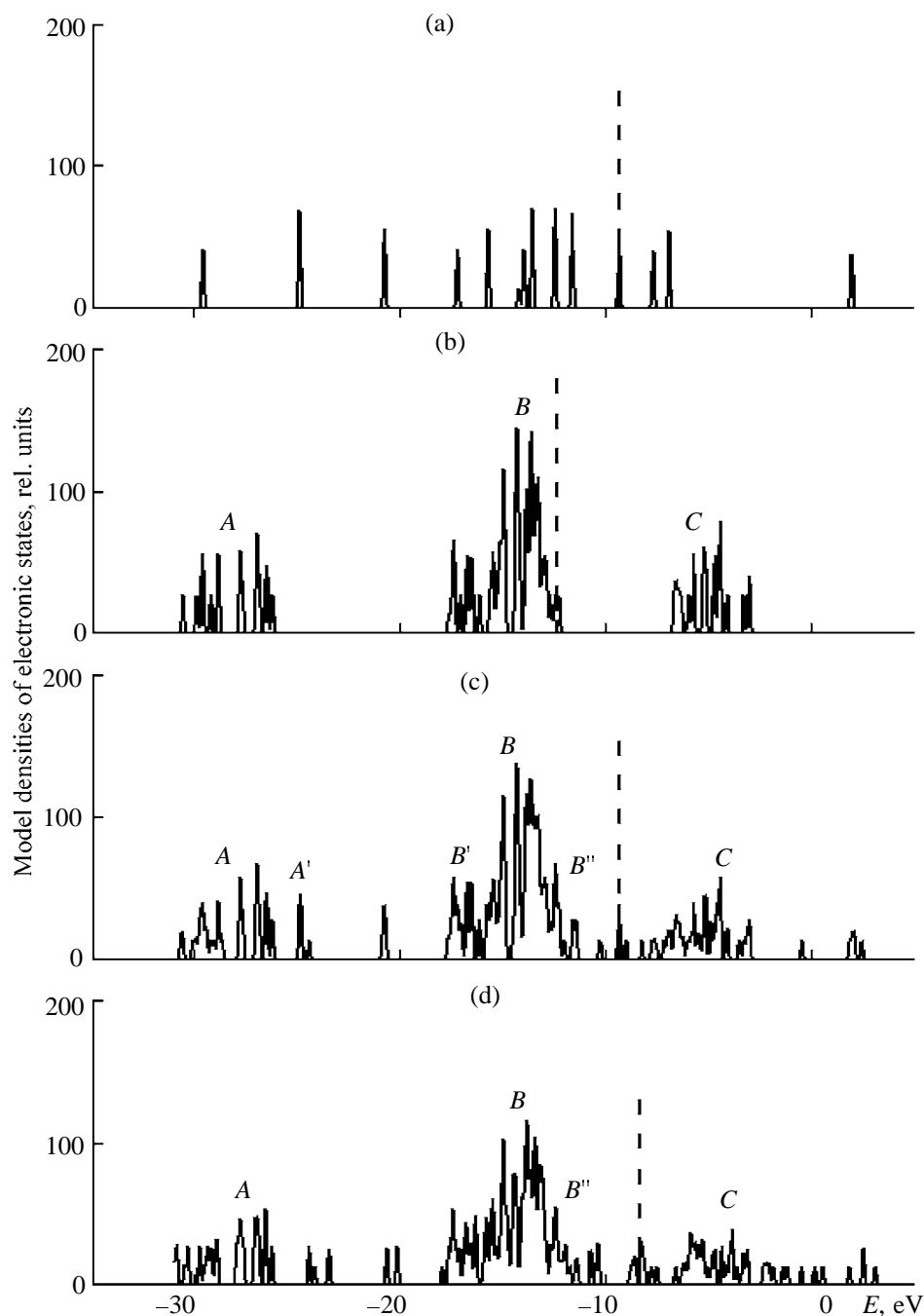


Fig. 2. Model density of electronic states: (a) $[C_{20}]_{\infty}$ chain, (b) (9,0)BN-NT, (c) $[C_{20}]_{\infty} + (9,0)BN\text{-}NT$ ad-system, and (d) $C_{20}@(9,0)BN\text{-}NT$ peapod (cell type III, Fig. 1). Here and in the other figures, the vertical lines denote the Fermi level.

nanotube interactions in atomic rings in nanotube walls, concentrically “embracing” fullerenes, make the overlap populations of B–N crystal orbitals lower than between neighboring molecules in nanotube sections. Consequently, fullerene intercalation results in formation of an anisotropic system of interatomic bonds along the tube with the “modulation” period determined by the chain period of fullerenes. Pre-

sumably, by varying mutual arrangement of fullerenes in the tube (for instance, by creating conditions for one-dimensional polymerization), one will be able to directionally vary the configuration of the overall “carcass” of chemical bonds in peapod shells and, as a result, affect the electronic and elastic properties of the whole system. Note that the “plasticization” of the $C_{60}@(10,10)C\text{-}NT$ peapod relative to the isolated

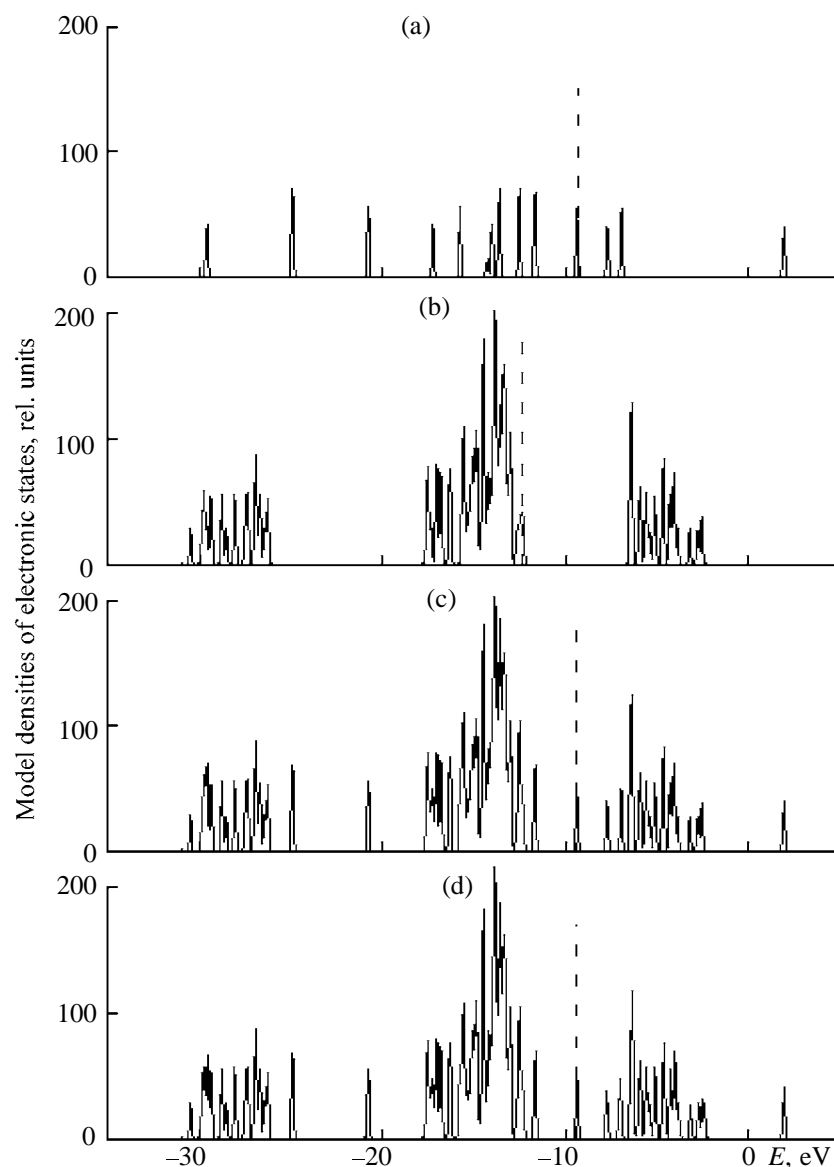


Fig. 3. Model density of electronic states: (a) $[C_{20}]_{\infty}$ chain, (b) (13,0)BN-NT, (c) $[C_{20}]_{\infty} + (13,0)$ BN-NT ad-system, and (d) $C_{20}@(13,0)$ BN-NT peapod.

nanotube has been established recently by Farajian and Mikami [15] in calculations of elasticity modules and Poisson coefficients.

The possibility of such polymerization follows from the calculations for the $C_{28}@(10,0)$ BN-NT peapod (Fig. 4) with C_{28} molecules spaced at about 0.2 nm. It was found that already in the isolated $[C_{20}]_{\infty}$ chain result interactions of neighboring molecules result in that the spectrum of this system differs from that of the free fullerene C_{28} [29]. Interactions of C_{28} with each other and with nanotube atoms enhance in the series $[C_{28}]_{\infty}$, $[C_{28}]_{\infty} + (10,0)$ BN-NT, $C_{28}@(10,0)$ BN-NT, giving rise to new hybrid

states in the spectra (Fig. 4, peaks B' , B'' , C' , and C''). These effects, in their turn, result in weakening of bonds between fullerene atoms [from ~ 1.03 for C_{28} to ~ 0.95 e/bond for the fullerenes in $C_{28}@(10,0)$ BN-NT], implying probability of structural relaxation of “ideal” C_{28} fullerenes and their coalescence in peapods.

Thus, in the present work we predicted new flexible quasi-one-dimensional structures, so-called peapods that consist of regular chains of the small fullerenes C_{20} and C_{28} encapsulated in boron–nitrogen nanotubes, and performed a quantum-chemical study of their electronic properties. It was found that the most active (crucial for interactions of C_{20} and C_{28}

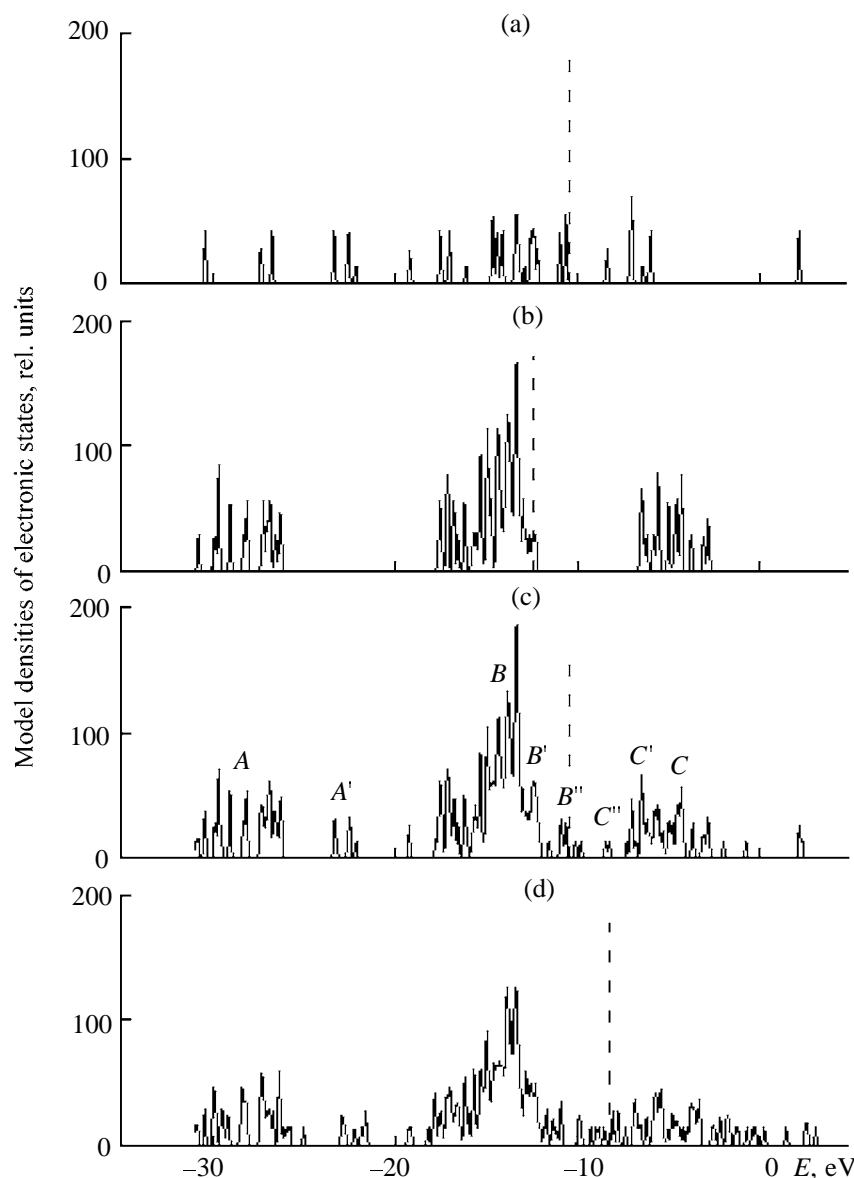


Fig. 4. Model densities of electronic states: (a) $[C_{28}]_{\infty}$ chain, (b) (10,0)BN-NT, (c) $[C_{28}]_{\infty} + (10,0)BN-NT$, and (d) $C_{28}@(10,0)BN-NT$ peapod (configuration I, Table 2).

with each other and with the nanotube) are outer partially occupied $C2p$ states of fullerenes. It was shown that in peapods with fullerene–nanotube distances longer than covalent bonds no new (hybrid) states are formed and the spectrum of the system is a superposition of the spectra of the “isolated” fullerene chain and nanotubes. The density of carriers is mostly localized on outer states of fullerenes, that form a narrow “impurity” band in the dielectric band of nanotubes whose semiconducting properties are preserved in peapods.

The spectra of peapods with fullerene–nanotube

distances characteristic of covalent bonds contain a set of electronic states associated with formation of new fullerene–nanotube and fullerene–fullerene bonds. Therewith, pair bonds defining the structure of the starting fullerenes get weaker, which suggests spontaneous polymerization inside nanotubes.

To conclude, an effective way of controlling the electronic properties of the peapods in hand is to vary the chemical composition of intercalated cage-like molecules. In this connection interesting objects for further research may be peapods involving endocomplexes of the basis of C_{28} fullerene, $M@C_{28}$ endo-

Table 2. Fermi energy (E_F , eV), total one-electron energies (E_{tot} , eV) and pair bond populations for boron–nitrogen nanotubes decorated by a chain of adsorbed fullerenes and for $C_{20}, C_{28}@BN\text{-NT}$ peapods^a

System	$-E_F$	$-E_{\text{tot}}$	Bond populations ^b	
			B–N (1)	B–N(2)
(9,0)BN–NT	12.296		0.768	
$C_{20}+(9,0)BN\text{-NT}$				
I	9.031	6534.37	0.760	0.765
II	9.119	6535.77	0.761	0.767
III	9.369	6568.83	0.762	0.768
IV	9.347	6567.63	0.765	0.768
$C_{20}@(9,0)BN\text{-NT}$				
I	8.640	6500.81	0.728	0.759
II	8.002	6509.10	0.719	0.754
III	8.314	6509.46	0.749	0.758
IV	8.341	6509.33	0.750	0.757
(10,0)BN–NT	12.292		0.770	
$C_{28}+(10,0)BN\text{-NT}$				
I	10.634	7714.41	0.765	0.770
II	10.337	7712.87	0.766	0.770
III	10.244	7712.50	0.765	0.770
IV	10.533	7713.60	0.763	0.770
$C_{28}@(10,0)BN\text{-NT}$				
I	8.087	7633.46	0.711	0.760
II	8.279	7631.82	0.708	0.756
III	7.551	7626.71	0.714	0.763
IV	7.820	7627.41	0.712	0.764

^a (I–IV) Configurations of fullerene–nanotube mutual arrangements (Fig. 1). ^b (1, 2) Bond populations in rings of B and N atoms, surrounding the fullerene, and between neighboring fullerenes, respectively.

fullerenes (M = Sc, Ti, Zr, Hf [29]). We suggest that intercalation into the bulk of nanotubes of these endo-complexes (along with the other type of metal–carbon nanoparticles, metallocarbohedrenes, we proposed in [19, 20]) may open the way to new unique nanotubular materials involving Group III–V *d*-metals.

Peapods formed by small fullerenes and carbon nanotubes hold no less promise, specifically as new superconductors.

Service [31] declared $C_{60}@C\text{-NT}$ as potential high-temperature superconductors. On the other hand, it is suggested [25, 32, 33] on the basis of calculated vibrational characteristics of small fullerenes and electron–phonon interactions in their molecular crystals (for instance, NaC_{22} [32] or A_3C_{28} [33], where A are alkali metals) that these molecules are more promising for design of high-temperature superconductors than

the “classical” C_{60} and C_{70} . Calculations of model nanostructures $C_{20}, C_{28}@(n,0)C\text{-NT}$ and $M@C_{28}@(n, 0)C$, BN–NT are presently in progress.

ACKNOWLEDGMENTS

The work was financially supported by the Russian Foundation for Basic Research (project no. 01-03-32513).

REFERENCES

1. Rakov, E.G., *Usp. Khim.*, 2001, vol. 70, no. 10, p. 934.
2. Ivanovskii, A.L., *Usp. Khim.*, 2002, vol. 71, no. 3, p. 203.
3. Smith, B.W., Monthieux, M., and Luzzi, D.E., *Nature*, 1998, vol. 396, no. 6709, p. 323.
4. Burteaux, B., Claye, A., Smith, B.W., Monthieux, M., Luzzi, D.E., and Fischer, J.E., *Chem. Phys. Lett.*, 1999, vol. 310, no. 1, p. 21.
5. Smith, B.W., Monthieux, M., and Luzzi, D.E., *Chem. Phys. Lett.*, 1999, vol. 315, nos. 1–2, p. 31.
6. Smith, B.W. and Luzzi, D.E., *Chem. Phys. Lett.*, 2000, vol. 321, nos. 1–2, p. 169.
7. Smith, B.W. and Luzzi, D.E., *Carbon*, 2000, vol. 38, nos. 11–12, p. 1751.
8. Bandow, S., Takizawa, M., Hirahara, K., Yudasaka, M., and Iijima, S., *Chem. Phys. Lett.*, 2001, vol. 337, nos. 1–3, p. 48.
9. Maniwa, Y., Kodama, T., Kikuchi, K., Hirahara, K., Suenaga, K., Iijima, S., Suzuki, S., Achiba, Y., and Kratschmer, W., *Synth. Metals*, 2001, vol. 121, nos. 1–3, p. 1195.
10. Liu, X., Pichler, T., Knupfer, A., Golden, M.S., Fink, J., Kataura, H., Achibam Y., Hirahara, K., and Iijima, S., *Phys. Rev. B*, 2002, vol. 6504, no. 4, p. 5419.
11. Hirahara, K., Bandow, S., Suenaga, K., Okazaki, T., Shinohara, H., and Iijima, S., *Phys. Rev. B*, 2001, vol. 6411, no. 11, p. 5420.
12. Hirahara, K., Suenaga, K., Bandow, S., Kato, H., Okazaki, T., Shinohara, H., and Iijima, S., *Phys. Rev. Lett.*, 2000, vol. 85, no. 25, p. 5384.
13. Hornbaker, D.J., Kahng, S.I., Misra, S., Smith, B.W., Johnsos, A.T., Mele, E.J., Luzzi, D.E., and Yazdani, A., *Science*, 2002, vol. 295, no. 5556, p. 828.
14. Okada, S., Saito, S., and Oshiyama, A., *Phys. Rev. Lett.*, 2001, vol. 86, no. 17, p. 3835.
15. Farajian, A.A. and Mikami, M., *J. Phys.: Condens. Matter.*, 2001, vol. 13, no. 7, p. 8049.
16. Chiu, P.W., Gu, G., Kim, G.T., Philipp, G., Roth, S.,

- Yang, S.F., and Yang, S., *Appl. Phys. Lett.*, 2001, vol. 79, no. 23, p. 3845.
17. Smith, B.W., Luzzi, D.E., and Achiba, Y., *Chem. Phys. Lett.*, 2000, vol. 331, nos. 2–4, p. 137.
18. Stefan, O., Bando, Y., Loiseau, A., Willaime, F., Shramachenko, N., Tamiya, T., and Sato, T., *Appl. Phys. A*, 1998, vol. 67, no. 1, p. 107.
19. Ivanovskaya, V.V., Sofronov, A.A., and Ivanovskii, A.L., *Teor. Eksp. Khim.*, 2001, vol. 37, no. 6, p. 331.
20. Sofronov, A.A., Ivanovskaya, V.V., Makurin, Yu.N., and Ivanovskii, A.L., *Chem. Phys. Lett.*, 2002, vol. 351, nos. 1–2, p. 35.
21. Goldschmidt, H.J., *Interstitial Alloys*, London: Butterworth, 1967.
22. Rohmer, M., Bernard, M., and Poblet J.-M., *Chem. Rev.*, 2000, vol. 10, no. 2, p. 495.
23. Cyvin, B.N., Brensdal, E., Brunvoll, J., and Cyvin, S.J., *J. Mol. Struct.*, 1995, vol. 352, p. 481.
24. Li, A. and Li, Q., *J. Mol. Struct. (Theochem)*, 1998, vol. 432, no. 2, p. 115.
25. Saito, M. and Miyamoto, Y., *Phys. Rev. Lett.*, 2001, vol. 87, no. 3, p. 5503.
26. Balerieius, L.M., Stumbrys, E., and Tamulis, A., *Fullerene Sci. Technol.*, 1997, vol. 5, no. 1, p. 85.
27. Choho, K., Van de Woude, G., Van Lier, G., and Geerlings, P., *J. Mol. Struct. (Theochem)*, 1997, vol. 417, no. 3, p. 265.
28. Mishra, R.K., Lin, Y.T., and Lee, S.L., *Int. J. Quantum Chem.*, 2001, vol. 84, no. 6, p. 642.
29. Makurin, Yu.N., Sofronov, A.A., Gusev, A.I., and Ivanovskii, A.L., *Chem. Phys.*, 2001, vol. 270, no. 3, p. 293.
30. Ivanovskii, A.L., *Kvantovaya khimiya v materialovedenii. Nanotubulyarnye formy veshchestva* (Quantum Chemistry in Material Science. Nanotubular Forms of Substance), Ekaterinburg: Ural Br. Russ. Akad. Nauk, 1999.
31. Service, R.F., *Science*, 2001, vol. 292, no. 5514, p. 45.
32. Spagnolatti, I., Bernasconi, M., and Bedenek, G., *Europhys. Lett.*, 2002, vol. 59, no. 4, p. 572.
33. Breda, N., Broglia, R.A., Colo, G., Onida, G., Provassi, D., and Vigezzi, E., *Phys. Rev. B*, 2000, vol. 62, no. 1, p. 130.